Mon. Not. R. Astron. Soc. **383,** 1079–1088 (2008) doi:10.1111/j.1365-2966.2007.12589.x

The evolution of massive black hole seeds

Marta Volonteri,[1⋆] Giuseppe Lodato[2] and Priyamvada Natarajan[3,4]

[1]*Department of Astronomy, University of Michigan, Ann Arbor, MI 48109, USA*
[2]*Department of Physics and Astronomy, University of Leicester, Leicester LE1 7RH*
[3]*Department of Astronomy, Yale University, PO Box 208101, New Haven, CT 06511-208101, USA*
[4]*Department of Physics, Yale University, PO Box 208120, New Haven, CT 06520-208120, USA*

Accepted 2007 October 15. Received 2007 October 12; in original form 2007 August 31

ABSTRACT

We investigate the evolution of high-redshift seed black hole masses at late times and their observational signatures. The massive black hole seeds studied here form at extremely high redshifts from the direct collapse of pre-galactic gas discs. Populating dark matter haloes with seeds formed in this way, we follow the mass assembly of these black holes to the present time using a Monte Carlo merger tree. Using this machinery, we predict the black hole mass function at high redshifts and at the present time, the integrated mass density of black holes and the luminosity function of accreting black holes as a function of redshift. These predictions are made for a set of three seed models with varying black hole formation efficiency. Given the accuracy of present observational constraints, all three models can be adequately fitted. Discrimination between the models appears predominantly at the low-mass end of the present-day black hole mass function which is not observationally well constrained. However, all our models predict that low surface brightness, bulgeless galaxies with large discs are least likely to be sites for the formation of massive seed black holes at high redshifts. The efficiency of seed formation at high redshifts has a direct influence on the black hole occupation fraction in galaxies at $z = 0$. This effect is more pronounced for low-mass galaxies. This is the key discriminant between the models studied here and the Population III remnant seed model. We find that there exist a population of low-mass galaxies that do not host nuclear black holes. Our prediction of the shape of the $M_{\rm BH}$–σ relation at the low-mass end is in agreement with the recent observational determination from the census of low-mass galaxies in the Virgo cluster.

Key words: black hole physics – galaxies: evolution – quasars: general – cosmology: miscellaneous.

1 INTRODUCTION

The demography of local galaxies suggests that most galaxies host a quiescent supermassive black hole (SMBH) at the present time and the properties of the black hole (BH) are correlated with those of the host spheroid. In particular, recent observational evidence points to the existence of a tight correlation between the mass of the central BH and the velocity dispersion of the host spheroid (Tremaine et al. 2002; Ferrarese & Merritt 2000; Gebhardt et al. 2000) in nearby galaxies. This correlation strongly suggests coeval growth of the BH and the stellar component via likely regulation of the gas supply in galactic nuclei (Silk & Rees 1998; Kauffmann & Haehnelt 2000; King 2003; Thompson, Quataert & Murray 2005).

BH growth is believed to be powered by gas accretion (Lynden-Bell 1969) and accreting BHs are detected as optically bright quasars. These optically bright quasars appear to exist out to the highest redshifts probed at the present time. Therefore, the mass build-up of SMBHs is likely to have commenced at extremely high redshifts ($z > 10$). In fact, optically bright quasars have now been detected at $z > 6$ (e.g. Fan et al. 2004, 2006) in the Sloan Digital Sky Survey (SDSS). Hosts of high-redshift quasars are often strong sources of dust emission (Omont et al. 2001; Carilli et al. 2002; Cox et al. 2002; Walter et al. 2003), suggesting that quasars were already in place in massive galaxies at a time when galaxies were undergoing vigourous star formation. The growth spurts of SMBHs are also seen in the X-ray waveband. The integrated emission from these X-ray quasars generates the cosmic X-ray background (XRB), and its spectrum suggests that most of the BH growth is obscured in optical wavelengths (Fabian & Iwasawa 1999; Mushotzky et al. 2000; Hasinger et al. 2001; Barger et al. 2003, 2005; Worsley et al. 2005). There exist examples of obscured BH growth in the form of 'Type-2' quasars, but their detected numbers are fewer than expected from models of the XRB. However, there is recent tantalizing evidence from infrared studies that dust-obscured accretion is ubiquitous (Martínez-Sansigre et al. 2005). This work suggests that

⋆E-mail: martav@umich.edu

while SMBHs might spend most of their lifetime in an optically dim phase, the bulk of mass growth occurs in the short-lived quasar stages.

The assembly of BH mass in the Universe has been tracked using optical quasar activity. The present phenomenological approach to understanding the assembly of SMBHs involves optical data from both high and low redshifts. These data are used as a starting point to construct a consistent picture that fits within the larger framework of the growth and evolution of structure in the Universe (Haehnelt, Natarajan & Rees 1998; Haiman & Loeb 1998; Kauffmann & Haehnelt 2000, 2002; Wyithe & Loeb 2002; Di Matteo et al. 2003; Volonteri, Haardt & Madau 2003).

Present modelling is grounded in the framework of the standard paradigm that involves the growth of structure via gravitational amplification of small perturbations in a cold dark matter (CDM) universe – a model that has independent validation, most recently from *Wilkinson Microwave Anisotropy Probe* (*WMAP*) measurements of the anisotropies in the cosmic microwave background (Page et al. 2003; Spergel et al. 2003). Structure formation is tracked in cosmic time by keeping a census of the number of collapsed dark matter haloes of a given mass that form; these provide the sites for harbouring BHs. The computation of the mass function of dark matter haloes is done using either the Press–Schechter (Press & Schechter 1974) or the extended Press–Schechter theory (Lacey & Cole 1993), or Monte Carlo realizations of merger trees (Kauffmann & Haehnelt 2000; Volonteri et al. 2003; Bromley, Somerville & Fabian 2004) or, in some cases, directly from cosmological *N*-body simulations (Di Matteo et al. 2003; Di Matteo, Springel & Hernquist 2005).

In particular, Volonteri et al. (2003) have presented a detailed merger-tree based scenario to trace the growth of BHs from the earliest epochs to the present day. Monte Carlo merger trees are created for present-day haloes and propagated back in time to a redshift of $\sim$20. With the merging history thus determined, the initial haloes at $z \sim 20$ are then populated with seed BHs which are assumed to be remnants of the first stars that form in the Universe. The masses of these so-called Population III stars are not accurately known; however, numerical simulations by various groups (Abel, Bryan & Norman 2000; Bromm, Coppi & Larson 2002) suggest that they are skewed to high masses of the order of a few hundred solar masses. Seeded with the end products of this first population, the merger sequence is followed and BHs are assumed to grow with every major merger episode. An accretion episode is assumed to occur as a consequence of every merger event. Following the growth and mass assembly of these BHs, it is required that the model is in consonance with the observed local $M_{\rm BH}$–σ relation. The luminosity function (LF) of quasars is predicted by these models and can be compared to observations. Volonteri et al. find that not every halo at high redshift needs to be populated with a BH seed in order to satisfy the observational constraints at $z = 0$. These models do not automatically reproduce the required abundance of SMBHs inferred to power the observed $z > 6$ SDSS quasars. In order to match the observation and produce SMBHs roughly 1 Gyr after the big bang, it is required that BHs undergo brief, but extremely strong growth episodes during which the accretion rate on to them is well in excess of the Eddington rate (Volonteri & Rees 2005; Begelman, Volonteri & Rees 2006). It is the existence of these SMBHs powering quasars at $z > 6$ that has prompted work on alternate channels to explain their mass build-up.

In order to alleviate the problem of explaining the existence of SMBHs in place by $z \sim 6$, roughly 1 Gyr after the big bang, in this paper we examine the possibility of using a well-motivated high-redshift seed BH mass function as the initial BH population at the highest redshifts. We investigate the effect of populating early dark matter haloes with massive BH seeds predicted in a model proposed by Lodato & Natarajan (2006, 2007). This model predicts a mass function for BHs that results from the direct collapse of pre-galactic gas discs. We study the implications of the use of this seed mass function versus that of the Population III remnants, in particular the difference in predictions at $z = 0$ for the massive seed models. In Section 2, we briefly outline the high-redshift BH seed formation model, and in Section 3 we evolve this model with redshift using the merger-tree formalism developed by Volonteri et al. (2003). The results are presented in Section 4, followed by a discussion of implications in the final section.

2 BLACK HOLE SEED FORMATION MODEL

In this paper, we track the formation of seed BHs in an *ab initio* model and follow their mass assembly down to $z = 0$. This is done in two separate phases – starting with the high-redshift seeds and tracing their subsequent growth. At high redshift ($z > 15$), we assume that the intergalactic medium has not been significantly enriched by metals, and therefore the gas cooling time-scales are long. Under these conditions, many authors (Koushiappas, Bullock & Dekel 2004; Begelman, Volonteri & Rees 2006; Lodato & Natarajan 2006, 2007) have shown that pre-galactic discs can efficiently transport matter into their innermost regions through the development and amplification of non-axisymmetric gravitational instabilities, often without fragmentation and star formation taking place (see below). This is the main seed formation phase, wherein massive seeds with $M \approx 10^5$–$10^6\,{\rm M}_\odot$ can form. At lower redshifts, cooling becomes more efficient and we assume that further accretion occurs via a 'merger-driven scenario' described in more detail in Section 3. In this section, we provide simple, analytical estimates of the amount of mass that we expect to be assembled in the form of massive BH seeds, based on the above scenario, as a function of the key dark matter halo parameters. Here, we refer in particular to the model by Lodato & Natarajan (2006), who considered the evolution of pre-galactic discs by self-consistently taking into account gravitational stability and fragmentation, thereby providing a detailed inventory of the fate of the gas.

Consider a dark matter halo of mass M and virial temperature $T_{\rm vir}$, containing gas mass $M_{\rm gas} = m_{\rm d}M$ (we also assume that the baryon fraction is roughly 5 per cent implying $m_{\rm d} = 0.05$), of primordial composition, that is, gas not enriched by metals, for which the cooling function is dominated by hydrogen. The other main parameter characterizing a dark matter halo that is relevant to the fate of the gas is its spin parameter $\lambda (\equiv J_{\rm h} E_{\rm h}^{1/2}/GM_{\rm h}^{5/2}$, where $J_{\rm h}$ is the total angular momentum and $E_{\rm h}$ is the binding energy). The distribution of spin parameters for dark matter haloes measured in numerical simulations is well fitted by a lognormal distribution in $\lambda_{\rm spin}$, with mean $\bar{\lambda}_{\rm spin} = 0.05$ and standard deviation $\sigma_\lambda = 0.5$:

$$p(\lambda)\,{\rm d}\lambda = \frac{1}{\sqrt{2\pi}\sigma_\lambda} \exp\left[-\frac{\ln^2(\lambda/\bar{\lambda})}{2\sigma_\lambda^2}\right] \frac{{\rm d}\lambda}{\lambda}. \quad (1)$$

This function has been shown to provide a good fit to the *N*-body results of several investigations (e.g. Warren et al. 1992; Cole & Lacey 1996; Bullock et al. 2001; van den Bosch et al. 2002).

If the virial temperature of the halo $T_{\rm vir} > T_{\rm gas}$, the gas collapses and forms a rotationally supported disc. For low values of the spin parameter λ the resulting disc can be compact and dense and is subject to gravitational instabilities. This occurs when the stability

parameter Q defined below approaches unity:

$$Q = \frac{c_s \kappa}{\pi G \Sigma} = \sqrt{2}\frac{c_s V_h}{\pi G \Sigma R}, \quad (2)$$

where R is the cylindrical radial coordinate, Σ is the surface mass density, c_s is the sound speed, $\kappa = \sqrt{2}V_h/R$ is the epicyclic frequency, and V_h is the circular velocity of the disc (mostly determined by the dark matter gravitational potential). We have also assumed that at the relevant radii ($\approx 10^2$–10^3 pc) the rotation curve is well described by a flat V_h profile. We consider here the earliest generations of gas discs, which are of pristine composition with no metals and therefore can cool only via hydrogen. In thermal equilibrium, if the formation of molecular hydrogen is suppressed, these discs are expected to be nearly isothermal at a temperature of a few thousand Kelvin (here we take $T_{gas} \approx 5000$ K, Lodato & Natarajan 2006). However, molecular hydrogen if present can cool these discs further down to temperatures of a few hundred Kelvin. The stability parameter has a critical value Q_c of the order of unity, below which the disc is unstable leading to the potential formation of a seed BH. The actual value of Q_c essentially determines how stable the disc is, with lower values of Q_c implying more stable discs. It is well known since Toomre (1964) proposed this stability criterion, that for an infinitesimally thin disc to be stable to fragmentation, $Q_c = 1$ for axisymmetric disturbances. The exact value of Q_c under more realistic conditions is not well determined. Finite thickness effects tend to stabilize the disc (reducing Q_c) while, on the other hand, non-axisymmetric perturbations are in reality more unstable (enhancing Q_c). Global, three-dimensional simulations of Keplerian discs (Lodato & Rice 2004, 2005) have shown that such discs settle down in a quasi-equilibrium configuration with Q remarkably close to unity, implying that the critical value $Q_c \approx 1$. In this paper, we take Q_c to be a free parameter and evaluate our results for a range of values.

If the disc becomes unstable, it develops non-axisymmetric spiral structures, which leads to an effective redistribution of angular momentum, thus feeding a growing seed BH in the centre. This process stops when the amount of mass transported to the centre, M_{BH}, is enough to make the disc marginally stable. This can be computed easily from the stability criterion in equation (2) and from the disc properties, determined from the dark matter halo mass and angular momentum (Mo, Mao & White 1998). In this way, we obtain that the mass accumulated in the centre of the halo is given by

$$M_{BH} = \begin{cases} m_d M \left[1 - \sqrt{\frac{8\lambda}{m_d Q_c}\left(\frac{j_d}{m_d}\right)\left(\frac{T_{gas}}{T_{vir}}\right)^{1/2}}\right] & \lambda < \lambda_{max} \\ 0 & \lambda > \lambda_{max} \end{cases} \quad (3)$$

where

$$\lambda_{max} = m_d Q_c / 8(m_d/j_d)(T_{vir}/T_{gas})^{1/2} \quad (4)$$

is the maximum halo spin parameter for which the disc is gravitationally unstable. Note that while $Q_c = 1$ provides the benchmark for the onset of instability, non-axisymmetric and global instabilities can cause the disc to become unstable for larger values of Q_c. For this reason, we investigate models with $1 < Q_c \leqslant 3$.

The process described above provides a means to transport matter from a typical scale of a few hundred parsecs down to radii of a few au. If the halo–disc system already possesses a massive BH seed from a previous generation, then this gas can provide a large fuel reservoir for its further growth. Note that the typical accretion rates implied by the above model are of the order of $0.01\,M_\odot\,yr^{-1}$, and are therefore sub-Eddington for seeds with masses of the order of $10^5\,M_\odot$ or so. If, on the other hand, no BH seed is present, then this large gas inflow can form a seed anew. The ultimate fate of the gas in this case at the smallest scales is more uncertain. One possibility, if the accretion rate is sufficiently large, has been described in detail by Begelman et al. (2006). The infalling material likely forms a quasi-star, the core of which collapses and forms a BH, while the quasi-star keeps accreting and growing in mass at a rate which would be super-Eddington for the central BH. Alternatively, the gas might form a supermassive star, which would eventually collapse and form a BH (Shapiro & Shibata 2002). There are no quantitative estimates of how much mass would ultimately end up collapsing in the hole. Thus, the BH seed mass estimates based on equation (3) should be considered as upper limits.

For large halo mass, the internal torques needed to redistribute the excess baryonic mass become too large to be sustained by the disc, which then undergoes fragmentation. This occurs when the virial temperature exceeds a critical value T_{max}, given by

$$\frac{T_{max}}{T_{gas}} > \left(\frac{4\alpha_c}{m_d}\frac{1}{1 + M_{BH}/m_d M}\right)^{2/3}, \quad (5)$$

where $\alpha_c \approx 0.06$ is a dimensionless parameter measuring the critical gravitational torque above which the disc fragments (Rice, Lodato & Armitage 2005).

To summarize, every dark matter halo is characterized by its mass M (or virial temperature T_{vir}) and by its spin parameter λ. The gas has a temperature $T_{gas} = 5000$ K. If $\lambda < \lambda_{max}$ (see equation 4) and $T_{vir} < T_{max}$ (equation 5), then we assume that a seed BH of mass M_{BH} given by equation (3) forms in the centre. The remaining relevant parameters are $m_d = 0.05, \alpha_c = 0.06$, and we consider three different values for $Q_c = 1.5$, 2 and 3, which will be referred to as (i) model A; (ii) model B and (iii) model C which correspond, respectively, to cases of increasing instability and therefore increasing efficiency for the formation of seed BHs. What we investigate in this paper are possible constraints/insights that the measured mass function of SMBHs at $z = 0$ can provide on the onset of instability and therefore on the efficiency of seed formation at extremely high redshifts.

To give an idea of the efficiency of BH seed formation at high z within the present model, we plot in Fig. 1, as an example, the probability of forming a BH (of any mass) at $z = 18$, as a function of halo mass, for the three models. It can be seen that typically up to 10 per cent of the haloes in the right mass range can form a central seed BH, the percentage rising to a maximum of $\approx$25 per cent for the high-efficiency model C (highly unstable discs), and dropping to a maximum of $\approx$4 per cent for the high-stability and therefore low-efficiency case (model A).

3 THE EVOLUTION OF SEED BHS

We follow the evolution of the MBH population resulting from the seed formation process delineated above in a ΛCDM universe. Our approach is similar to the one described in Volonteri et al. (2003). We simulate the merger history of present-day haloes with masses in the range $10^{11} < M < 10^{15}\,M_\odot$ starting from $z = 20$, via a Monte Carlo algorithm based on the extended Press–Schechter formalism.

Every halo entering the merger tree is assigned a spin parameter according to equation (1). Recent work on the fate of halo spins during mergers in cosmological simulations has led to conflicting results: Vitvitska et al. (2002) suggest that the spin parameter of a halo increases after a major merger, and the angular momentum decreases after a long series of minor mergers; D'Onghia & Navarro (2007)

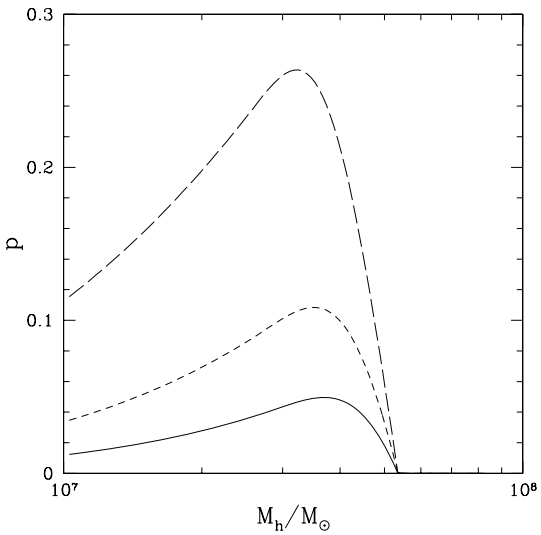

Figure 1. The probability of hosting a BH seed of any mass at $z = 18$ as a function of dark matter halo mass. The three curves refer to $Q_c = 1.5$ (low-efficiency case, solid line), $Q_c = 2$ (intermediate-efficiency case, short-dashed line) and $Q_c = 3$ (high-efficiency case, long-dashed line).

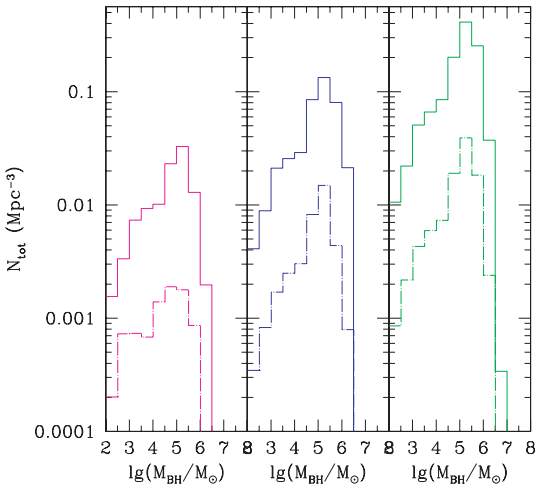

Figure 2. Mass function of MBH seeds in three Q-models that differ in seed formation efficiency. Left-hand panel: $Q_c = 1.5$ (the least-efficient model A), middle panel: $Q_c = 2$ (intermediate-efficiency model B), right-hand panel: $Q_c = 3$ (highly efficient model C). Seeds form at $z > 15$ and this channel ceases at $z = 15$. The solid histograms show the total mass function of seeds formed by $z = 15$, while the dashed histograms refer to seeds formed at a specific redshift, $z = 18$.

find instead no significant correlation between spin and merger history. Given the unsettled nature of this matter, we adopt Occam's razor to guide us, and assume that the spin parameter of a halo is not modified by its merger history.

When a halo enters the merger tree, we assign seed MBHs by determining if the halo meets all the requirements described in Section 2 for the formation of a central mass concentration. As we do not self-consistently trace the metal enrichment of the intergalactic medium, we consider here a sharp transition threshold, and assume that the MBH formation scenario suggested by Lodato & Natarajan ceases at $z \approx 15$ (see also Sesana et al. 2007; Volonteri et al., in preparation). At $z > 15$, therefore, whenever a new halo appears in the merger tree (because its mass is larger than the mass resolution), or a pre-existing halo modifies its mass by a merger, we evaluate if the gaseous component meets the conditions for efficient transport of angular momentum to create a large inflow of gas which can either form an MBH seed, or feed one if already present.

The efficiency of MBH formation is strongly dependent on critical value of the Toomre parameter Q_c, which sets the frequency of formation, and consequently the number density of MBH seeds. We investigate the influence of this parameter in the determination of the global evolution of the MBH population. Fig. 2 shows the number density of seeds formed in three models, with $Q_c = 1.5$ (low-efficiency model A), $Q_c = 2$ (intermediate-efficiency model B), and $Q_c = 3$ (high-efficiency model C). The solid histograms show the total mass function of seeds formed by $z = 15$ when this formation channel ceases, while the dashed histograms refer to seeds formed at a specific redshift slice at $z = 18$. The number of seeds changes by about one order of magnitude from the least-efficient to the most-efficient model, consistent with the probabilities shown in Fig. 1.

We assume that, after seed formation ceases, the $z < 15$ population of MBHs evolves according to a 'merger-driven scenario', as described in Volonteri, Salvaterra & Haardt (2006). We assume that during major mergers MBHs accrete gas mass that scales with the fifth power of the circular velocity (or equivalently the velocity dispersion σ_c) of the host halo (Ferrarese 2002). We thus set the final mass of the MBH at the end of the accretion episode to 90 per cent of the mass predicted by the M_{BH}–σ_c correlation, assuming that the scaling does not evolve with redshift. Major mergers are defined as mergers between two dark matter haloes with mass ratio between 1 and 10. BH mergers contribute to the mass increase of the remaining 10 per cent.

In order to calculate the accreting BH LF and to follow the BH mass growth during each accretion event, we also need to calculate the rate at which the mass, as estimated above, is accreted. This is assumed to scale with the Eddington rate for the MBH, and is based on the results of merger simulations, which heuristically track accretion on to a central MBH (Di Matteo et al. 2005; Hopkins et al. 2005a). The time spent by a given simulated active galactic nucleus (AGN) at a given bolometric luminosity[1] per logarithmic interval is approximated by (Hopkins et al. 2005b) as

$$\frac{\mathrm{d}t}{\mathrm{d}L} = |\alpha| t_Q \, L^{-1} \left(\frac{L}{10^9 \, \mathrm{L}_\odot} \right)^{\alpha}, \qquad (6)$$

where $t_Q \simeq 10^9$ yr, and $\alpha = -0.95 + 0.32 \log(L_{peak}/10^{12} \, \mathrm{L}_\odot)$. Here L_{peak} is the luminosity of the AGN at the peak of its activity. Hopkins et al. (2006) show that approximating L_{peak} with the Eddington luminosity of the MBH at its final mass (i.e. when it sits on the M_{BH}–σ_c relation) compared to computing the peak luminosity with equation (6) above gives the same result and in fact, the difference between these two cases is negligible. Volonteri et al. (2006) derive the following simple differential equation to express the instantaneous accretion rate (f_{Edd}, in units of the Eddington rate) for an MBH

[1] We convert accretion rate into luminosity assuming that the radiative efficiency equals the binding energy per unit mass of a particle in the last stable circular orbit. We associate the location of the last stable circular orbit to the spin of the MBHs, by self-consistently tracking the evolution of BH spins throughout our calculations (Volonteri et al. 2005). We set 20 per cent as the maximum value of the radiative efficiency, corresponding to a spin slightly below the theoretical limit for thin disc accretion (Thorne 1974).

of mass $M_{\rm BH}$ in a galaxy with velocity dispersion $\sigma_{\rm c}$:

$$\frac{{\rm d}f_{\rm Edd}(t)}{{\rm d}t} = \frac{f_{\rm Edd}^{1-\alpha}(t)}{|\alpha| t_Q} \left(\frac{\epsilon \dot{M}_{\rm Edd} c^2}{10^9\,{\rm L}_\odot} \right)^{-\alpha}, \quad (7)$$

where here t is the time elapsed from the beginning of the accretion event. Solving this equation gives us the instantaneous Eddington ratio for a given MBH at a specific time, and therefore we can self-consistently grow the MBH mass. We set the Eddington ratio $f_{\rm Edd} = 10^{-3}$ at $t = 0$. This same type of accretion is assumed to occur, at $z > 15$, following a major merger in which an MBH is not fed by disc instabilities.

In a hierarchical universe, where galaxies grow by mergers, MBH mergers are a natural consequence, and we trace their contribution to the evolving MBH population (cf. Sesana et al. 2007, for details on the dynamical modelling). During the final phases of an MBH merger, emission of gravitational radiation drives the orbital decay of the binary. Recent numerical relativity simulations suggest that merging MBH binaries might be subject to a large 'gravitational recoil': a general relativistic effect (Fitchett 1983; Redmount & Rees 1989) due to the non-zero net linear momentum carried away by gravitational waves in the coalescence of two unequal-mass BHs. Radiation recoil is a strong field effect that depends on the lack of symmetry in the system. For merging MBHs with high spin, in particular orbital configurations, the recoil velocity can be as high as a few thousands of kilometers per second (Campanelli et al. 2007a,b; González et al. 2007; Herrmann et al. 2007; Schnittman 2007). Here, we aim to determine the characteristic features of the MBH population deriving from a specific seed scenario, and its signature in present-day galaxies; we study the case without gravitational recoil. We discuss this issue further in Section 4.

4 RESULTS

Detection of gravitational waves from seeds merging at the redshift of formation (Sesana et al. 2007) is probably one of the best ways to discriminate among formation mechanisms. On the other hand, the imprint of different formation scenarios can also be sought in observations at lower redshifts. The various seed formation scenarios have distinct consequences for the properties of the MBH population at $z = 0$. Below, we present theoretical predictions of the various seed models for the properties of the local SMBH population.

4.1 SMBHs in dwarf galaxies

The repercussions of different initial efficiencies for seed formation for the overall evolution of the MBH population stretch from high redshift to the local Universe. Obviously, a higher density of MBH seeds implies a more numerous population of MBHs at later times, which can produce observational signatures in statistical samples. More subtly, the formation of seeds in a ΛCDM scenario follows the cosmological bias. As a consequence, the progenitors of massive galaxies (or clusters of galaxies) have a higher probability of hosting MBH seeds (cf. Madau & Rees 2001). In the case of low-bias systems, such as isolated dwarf galaxies, very few of the high-z progenitors have the deep potential wells needed for gas retention and cooling, a prerequisite for MBH formation. We can read off directly from Fig. 1 the average number of massive progenitors required for a present-day galaxy to host an MBH. In model A, a galaxy needs of the order of 25 massive progenitors (mass above $\sim 10^7\,{\rm M}_\odot$) to ensure a high probability of seeding within the merger tree. In model C, instead, the requirement drops to four massive progenitors, increasing the probability of MBH formation in lower bias haloes.

The signature of the efficiency of the formation of MBH seeds will consequently be stronger in isolated dwarf galaxies. Fig. 3 (bottom panel) shows a comparison between the observed $M_{\rm BH}$–σ relation and the one predicted by our models (shown with circles) and, in particular, from the left-hand to right-hand panel, the three models based on the Lodato & Natarajan (2006, 2007) seed masses with $Q_{\rm c} = 1.5$, 2 and 3, and a fourth model based on lower mass Population III star seeds. The upper panel of Fig. 3 shows the fraction of galaxies that do not host any MBHs for different velocity dispersion bins. This shows that the fraction of galaxies without an MBH increases with decreasing halo masses at $z = 0$. A larger fraction of low-mass haloes are devoid of central BHs for lower seed formation efficiencies. Note that this is one of the key discriminants between our models and those seeded with Population III remnants.

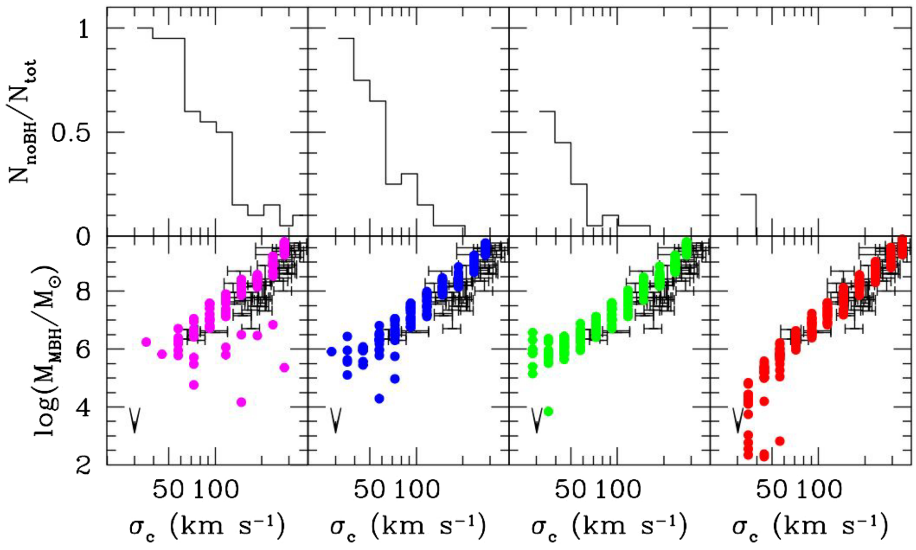

Figure 3. The $M_{\rm BH}$–velocity dispersion ($\sigma_{\rm c}$) relation at $z = 0$. Every circle represents the central MBH in a halo of given $\sigma_{\rm c}$. Observational data are marked by their quoted error bars, both in $\sigma_{\rm c}$ and in $M_{\rm BH}$ (Tremaine et al. 2002). Left-hand to right-hand panels: $Q_{\rm c} = 1.5$, $Q_{\rm c} = 2$, $Q_{\rm c} = 3$, Population III star seeds. Top panels: fraction of galaxies at a given velocity dispersion which do not host a central MBH.

As shown in Fig. 3, there are practically no galaxies without central BHs for the Population III seeds.

It is interesting to note that our model predictions are in very good agreement with the recent *HST* ACS census of BHs in low-mass galaxies in the Virgo cluster. Ferrarese et al. (2006) and Wehner & Harris (2006) suggest that below a transition galaxy mass ($\simeq 10^{10}\,M_\odot$) a central massive BH seems to be replaced by a nuclear star cluster. Although no definite proof that Virgo dwarfs are indeed without MBHs, the above results imply that MBHs are more common in large galactic systems. Our models also indicate that a minimum velocity dispersion exists, below which the probability of finding a central object is very low.

We make quantitative predictions for the local occupation fraction of MBHs. Our model A predicts that below $\sigma_c \approx 60\,\mathrm{km\,s^{-1}}$ the probability of a galaxy hosting an MBH is negligible. With increasing MBH formation efficiencies, the minimum mass for a galaxy that hosts an MBH decreases, and it drops below our simulation limits for model C. On the other hand, models based on lower mass Population III star remnant seeds, predict that MBHs might be present even in low-mass galaxies.

We note here that in our investigation we have not included any mechanism that could further lower the occupation fraction of MBHs (e.g. gravitational recoil, three-body MBH interactions). For any value of Q_c, the occupation fraction computed above is therefore an upper limit.

Although there are degeneracies in our modelling (e.g. between the minimum redshift for BH formation and instability criterion), the BH occupation fraction, and the masses of the BHs in dwarf galaxies are the key diagnostics. In local observations, the clearest signatures of massive seeds compared to Population III remnants, would be a lower limit of the order of the typical mass of seeds (Fig. 2) to the mass of MBHs in galaxy centres, as shown in Fig. 3. An additional caveat worth mentioning is the possibility that a galaxy is devoid of a central MBH because of dynamical ejections (due to either the gravitational recoil or three-body scattering). The signatures of such dynamical interactions should be more prominent in dwarf galaxies, but ejected MBHs would leave observational signatures on their hosts (Gültekin et al., in preparation). On top of that, Schnittman (2007) and Volonteri (2007) agree in considering the recoil a minor correction to the overall distribution of the MBH population at low redshift (cf. fig. 4 in Volonteri 2007).

Additionally, as MBH seed formation requires haloes with low angular momentum (low spin parameter), we envisage that low surface brightness, bulgeless galaxies with high spin parameters (i.e. large discs) are systems where MBH seed formation is less probable.[2] Furthermore, bulgeless galaxies are believed to preferentially have quieter merger histories and are unlikely to have experienced any major merger, which could have brought in an MBH from a companion galaxy. The (possible) absence of an MBH in M33 hence arises naturally (Gebhardt et al. 2001; Merritt, Ferrarese & Joseph 2001) in our model.

4.2 The LF of accreting BHs

Turning to the global properties of the MBH population, as suggested by Yu & Tremaine (2002) the mass growth of the MBH population at $z < 3$ is dominated by the mass accreted during the bright epoch of quasars, thus washing out most of the imprint of initial conditions. This is evident when we compute the LF of AGN. Clearly, the detailed shape of the predicted LF depends most strongly on the accretion prescription used. With our assumption that the gas mass accreted during each merger episode is proportional to V_c^5, we find that distinguishing between the various seed models is difficult. As shown in Fig. 4, all three models reproduce the bright end of the observed bolometric LF (Hopkins, Richards & Hernquist 2007) at higher redshifts (marked as the solid curve in all the panels), and predict a fairly steep faint end that is as yet undetected. All models fare less well at low redshift, shown in particular at $z = 0.5$. This could be due to the fact that we have used a single accretion prescription to model growth through epochs. On the other hand, the decline in the available gas budget at low redshifts (since the bulk of the gas has been consumed by this epoch by star formation activity) likely changes the radiative efficiency of these systems. Besides, observations suggest a sharp decline in the number of actively accreting BHs at low redshifts across wavelengths, produced most probably due to changes in the accretion flow as a result of change in the geometry of the nuclear regions of galaxies. In fact, all three of our models underpredict the slope at the faint end. There are three other effects that could cause this flattening of the LF at the faint end at low redshift for our models: (i) not having taken into account the fate of ongoing merging and the fate of satellite galaxies; (ii) the number of realizations generated and tracked is insufficient for statistics, as evidenced by the systematically larger error bars and (iii) more importantly, it is unclear if merger-driven accretion is indeed the trigger of BH fuelling in the low-redshift universe. We note that the three massive seed models and Population III seed model cannot be discriminated by the LF at high redshifts. Models B and C are also in agreement viz a viz the predicted BH mass function at $z = 6$ (see Fig. 2), even assuming a very high radiative efficiency (up to 20 per cent), while model A might need less-severe assumptions, in particular for BH masses larger than $10^7\,M_\odot$.

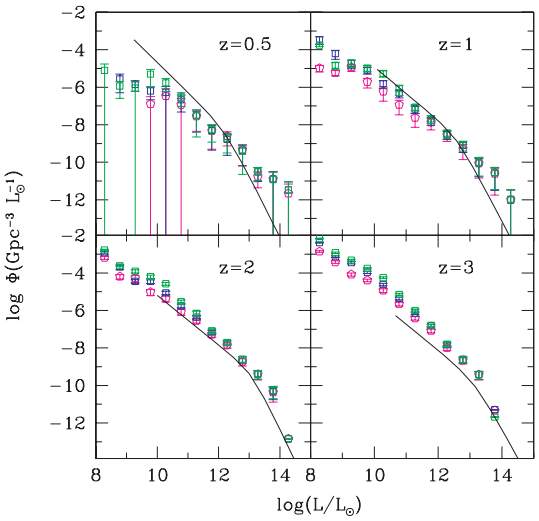

Figure 4. Bolometric LFs at different redshifts. All three models match the observed bright end of the LF at high redshifts and predict a steep slope at the faint end down to $z = 1$. The three models are not really distinguishable with the LF. However, at low redshifts, for instance, at $z = 0.5$, all three models are significantly flatter at both high and low luminosities and do not adequately match the present data. As discussed in the text, the LF is strongly determined by the accretion prescription and what we see here is simply a reflection of that fact.

[2] This prediction is pertinent to all models relying on gravitational instabilities triggered in low spin parameter haloes.

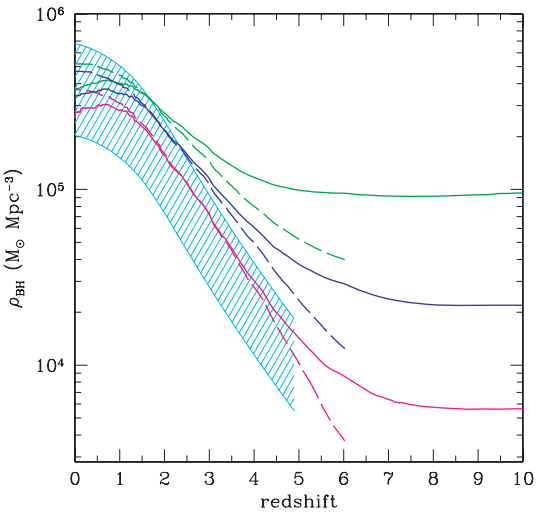

Figure 5. Integrated BH mass density as a function of redshift. Solid lines: total mass density locked into nuclear BHs. Dashed lines: integrated mass density accreted by BHs. Models based on BH remnants of Population III stars (lowest curve), $Q_c = 1.5$ (middle lower curve), $Q_c = 2$ (middle upper curve), $Q_c = 3$ (upper curve). Shaded area: constraints from Sołtan-type arguments, where we have varied the radiative efficiency from a lower limit of 6 per cent (applicable to Schwarzschild MBHs, upper envelope of the shaded area), to about 20 per cent (Wang et al. 2006). All three massive seed formation models are in comfortable agreement with the mass density obtained from integrating the optical LFs of quasars.

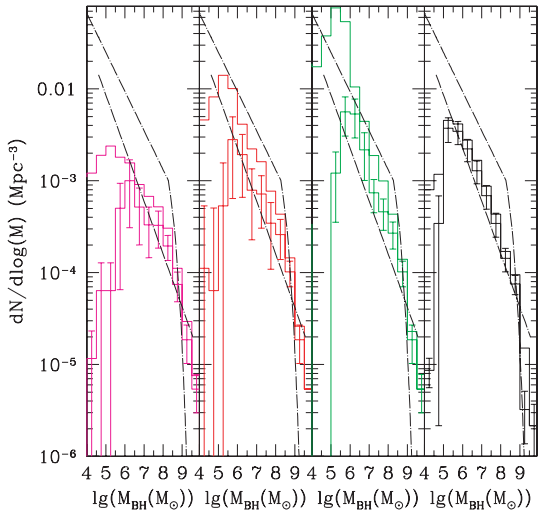

Figure 6. Mass function of BHs at $z = 0$. The histograms represent the results of our models, including central galaxies only (lower histograms with error bars), or including satellites in groups and clusters (upper histograms). Left-hand panel: $Q_c = 1.5$, middle left-hand panel: $Q_c = 2$, middle right-hand panel: $Q_c = 3$, right-hand panel: models based on BH remnants of Population III stars. Upper dashed line: mass function derived from combining the velocity dispersion function of Sloan galaxies (Sheth et al. 2003, where we have included the late-type galaxies extrapolation), and BH mass–velocity dispersion correlation (e.g. Tremaine et al. 2002). Lower dashed line: mass function derived using the Press–Schechter formalism from Jenkins et al. (2001) in conjunction with the M_{BH}–σ relation (Ferrarese 2002).

4.3 Comoving mass density of BHs

Since during the quasar epoch MBHs increase their mass by a large factor, signatures of the seed formation mechanisms are likely more evident at *earlier epochs*. We compare in Fig. 5 the integrated comoving mass density in MBHs to the expectations from Sołtan-type arguments (F. Haardt, private communication), assuming that quasars are powered by radiatively efficient flows (for details, see Yu & Tremaine 2002; Elvis, Risaliti & Zamorani 2002; Marconi et al. 2004). While during and after the quasar epoch, the mass densities in models A, B and C differ by less than a factor of 2, at $z > 3$ the differences become more pronounced.

A very efficient seed MBH formation scenario can lead to a very large BH density at high redshifts. For instance, for the highest-efficiency model C with $Q_c = 3$, the integrated MBH density at $z = 10$ is already ∼25 per cent of the density at $z = 0$. The plateau at $z > 6$ is due to our choice of scaling the accreted mass with the $z = 0\, M_{BH}$–velocity dispersion relation. Since in our models we let MBHs accrete a mass which scales with the fifth power of the circular velocity of the halo, the accreted mass is a small fraction of the MBH mass (see the discussion in Marulli et al. 2006), and the overall growth remains small, as long as the mass of the seed is larger than the accreted mass which, in our assumed scaling, happens when the mass of the halo is below a few times $10^{10}\,M_\odot$. The comoving mass density, an integral constraint, is reasonably well determined out to $z = 3$ but is poorly known at higher redshifts. All models appear to be satisfactory and consistent with present observational limits (shown as the shaded area).

4.4 BH mass function at $z = 0$

One of the key diagnostics is the comparison of the measured and predicted BH mass function at $z = 0$ for our three models. In Fig. 6, we show (from the left-hand to right-hand panel, respectively) the mass function predicted by models A, B and C and Population III remnant seeds compared to that obtained from measurements. The histograms show the mass function obtained with our models (where the upper histogram includes all the BHs while the lower one only includes BHs found in central galaxies of haloes in the merger tree approach). The two lines are two different estimates of the observed BH mass function. In the upper one, the measured velocity dispersion function for nearby late- and early-type galaxies from SDSS (Bernardi et al. 2003; Sheth et al. 2003) has been convolved with the measured M_{BH}–σ relation. We note here that the scatter in the M_{BH}–σ relation is not explicitly included in this treatment; however, the inclusion of the scatter is likely to preferentially affect the high-mass end of the black hole mass function, which provides stronger constraints on the accretion histories rather than the seed masses. It has been argued (e.g. Bernardi et al. 2007; Lauer et al. 2007; Tundo et al. 2007) that the BH mass function differs if the bulge mass is used instead of the velocity dispersion in relating the BH mass to the host galaxy. Since our models do not trace the formation and growth of stellar bulges in detail, we are restricted to using the velocity dispersion in our analysis.

The lower dashed curve is an alternate theoretical estimate of the BH mass function derived using the Press–Schechter formalism from Jenkins et al. (2001) in conjunction with the observed M_{BH}–σ relation. Selecting only the central galaxies of haloes in the merger tree approach adopted here (lower histograms) is shown to be fairly equivalent to this analytical estimate, and this is clearly borne out as is evident from the plot. When we include BHs in satellite galaxies (upper histograms, cf. the discussion in Volonteri et al. 2003), the predicted mass function moves towards the estimate based on SDSS galaxies. The higher efficiency models clearly produce more BHs. At higher redshifts, for instance, at $z = 6$, the mass functions of

active MBHs predicted by all models are in very good agreement, in particular for BH masses larger than 10^6 $M_\odot$, as it is the growth by accretion that dominates the evolution of the population. At the highest-mass end ($>10^9$ $M_\odot$) model A lags behind models B and C, although we stress once again that our assumptions for the accretion process are very conservative.

The *relative* differences between models A, B and C at the low-mass end of the mass function, however, are genuinely related to the MBH seeding mechanism (see also Figs 3 and 5). In model A, simply, fewer galaxies host an MBH, hence reducing the overall number density of BHs. Although our simplified treatment does not allow robust quantitative predictions, the presence of a 'bump' at $z = 0$ in the MBH mass function at the characteristic mass that marks the peak of the seed mass function (cf. Fig. 2) is a sign of highly efficient formation of massive seeds (i.e. much larger mass with respect to, for instance, Population III remnants). The higher the efficiency of seed formation, the more pronounced is the bump (note that the bump is most prominent for model C). Since present measurements of MBH masses extend barely down to $M_{\rm BH} \sim 10^6$ $M_\odot$, this feature cannot be observationally tested with present data but future campaigns, with the Giant Magellan Telescope or JWST, are likely to extend the mass function measurements to much lower BH masses.

5 DISCUSSION AND IMPLICATIONS

In this paper, we have investigated the role that the choice of the initial seed BH mass function at high redshift ($z \sim 18$) plays in the determination of observed properties of local quiescent SMBHs. While the errors on mass determinations of local BHs are large at the present time, definite trends with host galaxy properties are observed. The tightest correlation appears to be between the BH mass and the velocity dispersion of the host spheroid. Starting with the *ab initio* BH seed mass function computed in the context of direct formation of central objects from the collapse of pre-galactic discs in high-redshift haloes, we follow the assembly history to late times using a Monte Carlo merger tree approach. Key to our calculation of the evolution and build-up of mass is the prescription that we adopt for determining the precise mass gain during a merger. Motivated by the phenomenological observation of $M_{\rm BH} \propto V_{\rm c}^5$, we assume that this proportionality carries over to the gas mass accreted in each step. With these prescriptions, a range of predictions can be made for the mass function of BHs at high and low z, and the integrated mass density of BHs, all of which are observationally determined. We evolve three models, designated models A, B and C which correspond to increasing efficiencies, respectively, for the formation of seeds at high redshift. These models are compared to one in which the seeds are remnants of Population III stars.

It is important to note here that one major uncertainty prevents us from making more concrete predictions: the unknown metal-enrichment history of the Universe. Key to the implementation of our models is the choice of redshift at which massive seed formation is quenched. The direct seed formation channel described here ceases to operate once the Universe has been enriched by metals that have been synthesized after the first generation of stars have gone supernova. Once metals are available in the intergalactic medium gas cooling is much more efficient and hydrogen in either atomic or molecular form is no longer the key player. In this work, we have assumed this transition redshift to be $z = 15$. The efficiency of MBH formation and the transition redshift are somehow degenerate (e.g. a model with $Q = 1.5$ and enrichment redshift $z = 12$ is half-way between models A and B); if other constraints on this redshift were available, we could considerably tighten our predictions.

Below we list our predictions and compare how they fare with respect to present observations. The models investigated here clearly differ in predictions at the low-mass end of the BH mass function. With future observational sensitivity in this domain, these models can be distinguished.

Our model for the formation of relatively high mass BH seeds in high-z haloes has direct influence on the BH occupation fraction in galaxies at $z = 0$. This effect is more pronounced for low-mass galaxies. We find that a significant fraction of low-mass galaxies might not host a nuclear BH. This is in very good agreement with the shape of the $M_{\rm BH}$–σ relation determined recently from an observational census (an *HST* ACS survey) of low-mass galaxies in the Virgo cluster reported by Ferrarese et al. (2006).

The models studied here (with different BH seed formation efficiency) are distinguishable at the low-mass end of the BH mass function, while at the high-mass end the effect of initial seeds appears to be subdominant. While present data on the low-mass regime are scant (Barth et al. 2004; Greene & Ho 2007), future instruments and surveys are likely to probe this region of parameter space with significantly higher sensitivity.

All our models predict that low surface brightness, bulgeless galaxies with high spin parameters (i.e. large discs) are systems where MBH formation is least probable.

One of the key caveats of our picture is that it is unclear if the differences produced by different seed models on observables at $z = 0$ might be compensated or masked by BH fuelling modes at earlier epochs. There could be other channels for BH growth that dominate at low redshifts like minor mergers, dynamical instabilities, accretion of molecular clouds, tidal disruption of stars. The decreased importance of the merger-driven scenario is patent from observations of low-redshift AGN, which are for the large majority hosted by undisturbed galaxies (e.g. Pierce et al. 2007, and references therein) in low-density environments (e.g. Li et al. 2006). However, the feasibility and efficiency of some alternative channels are still to be proven (e.g. about the efficiency of feeding from large-scale instabilities, see discussion in Shlosman, Frank & Begelman 1989; Collin & Zahn 1999; Goodman 2003; King & Pringle 2007). In any event, while these additional channels for BH *growth* can modify the detailed shape of the mass function of MBHs, or of the LF of quasars, they will not create a new MBH. The occupation fraction of MBHs (see Fig. 3) is therefore largely *independent* of the accretion mechanism and a true signature of the formation process.

To date, most theoretical models for the evolution of MBHs in galaxies do not include *how* MBHs form. This work is a first analysis of the observational signatures of MBH formation mechanisms in the low-redshift universe, complementary to the investigation by Sesana et al. (2007), where the focus was on detection of seeds at the very early times where they form, via gravitational waves emitted during MBH mergers. We focus here on possible dynamical signatures that forming massive BH seeds carry over to the local Universe. We believe that the signatures of seed formation mechanisms will be far more clear if considered jointly with the evolution of the spheroids that they host. The mass, and especially the frequency, of the forming MBH seeds is a necessary input when investigating how the feedback from accretion on to MBHs influences the host galaxy, and is generally introduced in numerical models using extremely simplified, ad hoc prescriptions (e.g. Croton et al. 2005; Di Matteo et al. 2005; Springel et al. 2005; Bower et al. 2006; Cattaneo et al. 2006; Hopkins et al. 2006). Adopting more detailed models for BH

seed formation, as outlined here, can, in principle, strongly affect such results. For instance, Kauffmann et al. (2004) find that AGN activity is typically confined to galaxies with $M > 10^{10}$ $M_{\odot}$. If we consider the occupation fraction of MBHs in such galaxies, we find that it differs by a large factor between models A and C, being of the order of 10 per cent in the low-efficiency model (at $z \sim 1$–4) and 50 per cent or higher in model C. Consequently, the possibility of AGN feedback and its effect on the host would be selective in the former case, or widespread in the latter case. Adopting sensible assumptions for the masses, and frequency of MBH seeds in models of galaxy formation is necessary if we want to understand the symbiotic growth of MBHs and their hosts.

ACKNOWLEDGMENTS

PN and MV acknowledge the 2006 KITP programme titled 'The Physics of Galactic Nuclei', supported in part by the National Science Foundation under Grant No. PHY99-07949.

REFERENCES

Abel T., Bryan G. L., Norman M. L., 2000, ApJ, 540, 39
Barger A. J. et al., 2003, AJ, 126, 632
Barger A. J., Cowie L. L., Mushotzky R. F., Yang Y., Wang W.-H., Steffen A. T., Capak P., 2005, AJ, 129, 578
Barth A. J., Ho L. C., Rutledge R. E., Sargent W. L. W., 2004, ApJ, 607, 90
Begelman M. C., Volonteri M., Rees M. J., 2006, MNRAS, 370, 289
Bernardi M. et al., 2003, AJ, 125, 1882
Bernardi M., Sheth R. K., Tundo E., Hyde J. B., 2007, ApJ, 660, 267
Bower R. G., Benson A. J., Malbon R., Helly J. C., Frenk C. S., Baugh C. M., Cole S., Lacey C. G., 2006, MNRAS, 370, 645
Bromley J. M., Somerville R. S., Fabian A. C., 2004, MNRAS, 350, 456
Bromm V., Coppi P. S., Larson R. B., 2002, ApJ, 564, 23
Bullock J. S., Dekel A., Kolatt T. S., Kravtsov A. V., Klypin A. A., Porciani C., Primack J. R., 2001, ApJ, 555, 240
Campanelli M., Lousto C., Zlochower Y., Merritt D., 2007a, ApJ, 659, L5
Campanelli M., Lousto C. O., Zlochower Y., Merritt D., 2007b, Phys. Rev. Lett., 98, 231102
Carilli C. L. et al., 2002, AJ, 123, 1838
Cattaneo A., Dekel A., Devriendt J., Guiderdoni B., Blaizot J., 2006, MNRAS, 370, 1651
Cole S., Lacey C., 1996, MNRAS, 281, 716
Collin S., Zahn J. P., 1999, A&A, 344, 433
Cox P. et al., 2002, A&A, 387, 406
Croton D. J. et al., 2005, MNRAS, 356, 1155
Di Matteo T., Croft R. A. C., Springel V., Hernquist L., 2003, ApJ, 593, 56
Di Matteo T., Springel V., Hernquist L., 2005, Nat, 433, 604
D'Onghia E., Navarro J. F., 2007, MNRAS, 380, 58
Elvis M., Risaliti G., Zamorani G., 2002, ApJ, 565, L75
Fabian A. C., Iwasawa K., 1999, MNRAS, 303, L34
Fan X. et al., 2004, AJ, 128, 515
Fan X. et al., 2006, AJ, 131, 1203
Ferrarese L., 2002, ApJ, 578, 90
Ferrarese L. et al., 2006, ApJS, 164, 334
Ferrarese L., Merritt D., 2000, ApJ, 539, 9
Fitchett M. J., 1983, MNRAS, 203, 1049
Gebhardt K. et al., 2000, AJ, 119, 1157
Gebhardt K. et al., 2001, AJ, 122, 2469
González J. A., Sperhake U., Brügmann B., Hannam M., Husa S., 2007, Phys. Rev. Lett., 98, 091101
Goodman J., 2003, MNRAS, 339, 937
Greene J. E., Ho L. C., 2007, ApJ, 670, 92
Haehnelt M. G., Natarajan P., Rees M. J., 1998, MNRAS, 300, 817
Haiman Z., Loeb A., 1998, ApJ, 503, 505
Hasinger G. et al., 2001, A&A, 365, L45
Herrmann F., Hinder I., Shoemaker D. M., Laguna P., Matzner R. A., 2007, Phys. Rev. D, 76, 4032
Hopkins P. F., Hernquist L., Cox T. J., Di Matteo T., Robertson B., Springel V., 2005a, ApJ, 630, 716
Hopkins P. F., Hernquist L., Cox T. J., Di Matteo T., Robertson B., Springel V., 2005b, ApJ, 632, 81
Hopkins P. F., Hernquist L., Cox T. J., Di Matteo T., Robertson B., Springel V., 2006, ApJS, 163, 1
Hopkins P. F., Richards G. T., Hernquist L., 2007, ApJ, 654, 731
Jenkins A., Frenk C. S., White S. D. M., Colberg J. M., Cole S., Evrard A. E., Couchman H. M. P., Yoshida N., 2001, MNRAS, 321, 372
Kauffmann G., Haehnelt M., 2000, MNRAS, 311, 576
Kauffmann G., Haehnelt M. G., 2002, MNRAS, 332, 529
Kauffmann G., White S. D. M., Heckman T. M., Ménard B., Brinchmann J., Charlot S., Tremonti C., Brinkmann J., 2004, MNRAS, 353, 713
King A., 2003, ApJ, 596, L27
King A. R., Pringle J. E., 2007, MNRAS, 377, L25
Koushiappas S. M., Bullock J. S., Dekel A., 2004, MNRAS, 354, 292
Lacey C., Cole S., 1993, MNRAS, 262, 627
Lauer T. R. et al., 2007, ApJ, 662, 808
Li C., Kauffmann G., Wang L., White S. D. M., Heckman T. M., Jing Y. P., 2006, MNRAS, 373, 457
Lodato G., Natarajan P., 2006, MNRAS, 371, 1813
Lodato G., Natarajan P., 2007, MNRAS, 377, L64
Lodato G., Rice W. K. M., 2004, MNRAS, 351, 630
Lodato G., Rice W. K. M., 2005, MNRAS, 358, 1489
Lynden-Bell D., 1969, Nat, 223, 690
Madau P., Rees M. J., 2001, ApJ, 551, L27
Marconi A., Risaliti G., Gilli R., Hunt L. K., Maiolino R., Salvati M., 2004, MNRAS, 351, 169
Martínez-Sansigre A., Rawlings S., Lacy M., Fadda D., Marleau F. R., Simpson C., Willott C. J., Jarvis M. J., 2005, Nat, 436, 666
Marulli F., Crociani D., Volonteri M., Branchini E., Moscardini L., 2006, MNRAS, 368, 1269
Merritt D., Ferrarese L., Joseph C. L., 2001, Sci, 293, 1116
Mo H. J., Mao S., White S. D. M., 1998, MNRAS, 295, 319
Mushotzky R. F., Cowie L. L., Barger A. J., Arnaud K. A., 2000, Nat, 404, 459
Omont A., Cox P., Bertoldi F., McMahon R. G., Carilli C., Isaak K. G., 2001, A&A, 374, 371
Page L. et al., 2003, ApJS, 148, 233
Pierce C. M. et al., 2007, ApJ, 660, L19
Press W. H., Schechter P., 1974, ApJ, 187, 425
Redmount I. H., Rees M. J., 1989, Comments Astrophys., 14, 165
Rice W. K. M., Lodato G., Armitage P. J., 2005, MNRAS, 364, L56
Schnittman J. D., 2007, ApJ, 667, L133
Sesana A., Volonteri M., Haardt F., 2007, MNRAS, 377, 1711
Shapiro S. L., Shibata M., 2002, ApJ, 577, 904
Sheth R. K. et al., 2003, ApJ, 594, 225
Shlosman I., Frank J., Begelman M. C., 1989, Nat, 338, 45
Silk J., Rees M. J., 1998, A&A, 331, L1
Spergel D. N. et al., 2003, ApJS, 148, 175
Springel V. et al., 2005, Nat, 435, 629
Thompson T. A., Quataert E., Murray N., 2005, ApJ, 630, 167
Thorne K. S., 1974, ApJ, 191, 507
Toomre A., 1964, ApJ, 139, 1217
Tremaine S. et al., 2002, ApJ, 574, 740
Tundo E., Bernardi M., Hyde J. B., Sheth R. K., Pizzella A., 2007, ApJ, 663, 53
van den Bosch F. C., Abel T., Croft R. A. C., Hernquist L., White S. D. M., 2002, ApJ, 576, 21
Vivitska M., Klypin A. A., Kravtsov A. V., Wechsler R. H., Primack J. R., Bullock J. S., 2002, ApJ, 581, 799
Volonteri M., 2007, ApJ, 663, L5
Volonteri M., Rees M. J., 2005, ApJ, 633, 624
Volonteri M., Haardt F., Madau P., 2003, ApJ, 582, 559
Volonteri M., Madau P., Quataert E., Rees M. J., 2005, ApJ, 620, 69
Volonteri M., Salvaterra R., Haardt F., 2006, MNRAS, 373, 121

Walter F. et al., 2003, Nat, 424, 406
Wang J.-M., Chen Y.-M., Ho L. C., McLure R. J., 2006, ApJ, 642, 111
Warren M. S., Quinn P. J., Salmon J. K., Zurek W. H., 1992, ApJ, 399, 405
Wehner E. H., Harris W. E., 2006, ApJ, 644, L17
Worsley M. A. et al., 2005, MNRAS, 357, 1281
Wyithe J. S. B., Loeb A., 2002, ApJ, 581, 886
Yu Q., Tremaine S., 2002, MNRAS, 335, 965

This paper has been typeset from a TEX/LATEX file prepared by the author.